

Induction Motors Thermal Analysis

Dave STATON¹⁾ and Livio ŠUŠNJIĆ²⁾

1) Motor Design Ltd., 4 Scotland Street,
Ellesmere, Shropshire, UK, SY12 0EG
United Kingdom

2) Tehnički fakultet Sveučilišta u Rijeci (Faculty
of Engineering University of Rijeka),
Vukovarska 58, HR - 51000 Rijeka,
Republic of Croatia

livio.susnjic@riteh.hr

Keywords

*Heat transfer
Induction motors
Thermal analyses
Thermal model*

Ključne riječi

*Asinkroni strojevi
Prijenos topline
Toplinska analiza
Toplinski model*

Received (primljeno): 2009-09-20

Accepted (prihvaćeno): 2009-10-30

1. Introduction

A motor's performance is governed by its electromagnetic and thermal design. Both designs are in fact interrelated. Not only are the losses dependant on the temperatures and vice-versa, but more complex issues arise at the design stage. Examples of such complexities are the fact that it is usually easier to dissipate stator iron loss than copper loss due to its closer proximity to the housing; lower loss lamination materials have reduced thermal conductivities; the end-winding losses have local air cooling (or conductive cooling if potted); etc. More recently it has been discovered that attention to the thermal design can be rewarded by major improvements in the overall performance. The rise in awareness of the importance of thermal issues has lead to an increased amount of work devoted to the development of electric motor thermal models. Previous papers [1-4] review a number of these difficult design aspects and gives advice on how to deal with them when developing design

Original scientific paper

The temperature distribution over the cross-section of an induction motor is calculated at the steady state and transient condition. In order to develop smaller and more efficient electric motors, there is a necessity to carry out more thermal analysis in parallel with the traditional electromagnetic design. It has been found that attention to the thermal design can be rewarded by major improvements in the overall performance. The developed thermal model for Total Enclosed Fan Cooled (TEFC) induction motors is implemented into the design program called Motor-CAD™. The model produced has been experimentally verified by measurements on industrial machines. The obtained results confirm that the developed thermal model is capable of a sufficient degree of accuracy in the thermal design of (TEFC) induction motors.

Toplinska analiza asinkronog stroja

Izvorno znanstveni članak

Predstavljen je proračun razdiobe temperature po presjeku asinkronog stroja za stacionarno opterećenje kao i za slučaj zakočenog rotora. U cilju smanjenja dimenzija i povećanja korisnosti neophodno je primijeniti detaljniju toplinsku analizu uz elektromagnetski proračun. Nalazi se da je rezultat primjene detaljnije toplinske analize poboljšanje operativnih karakteristika motora. Razvijeni toplinski model za potpuno zatvoreni asinkroni motor s prisilnim hlađenjem zrakom izvana (TEFC) je uključen u računalni program za projektiranje naziva Motor-CAD™. Prikazani model je eksperimentalno potvrđen na industrijskim električnim strojevima. Dobiveni rezultati potvrđuju da razvijeni toplinski model posjeduje dovoljan stupanj točnosti u toplinskom projektiranju (TEFC) asinkronih strojeva.

algorithms suitable for inclusion in thermal lumped circuit models.

The problems emphasized in these papers are:

- interference gaps between components,
- winding models suitable for identifying hot-spots and accounting for non-perfect impregnation,
- convection cooling from the surface of the machine including problems of open axial channel fin leakage and blockage (due to lugs and terminal boxes),
- turbulent cooling around the end-winding and axial end sections of the machine including fanning effects of induction motor wafers,
- heat transfer across the airgap,
- uncertainty of material property data and
- bearing and end-shield models.

This paper gives a synthesis of previously published papers [1-4, 6] and experimental verification of the proposed thermal model of the induction machine.

Symbols/Oznake

$R_{cu,ir}$	- thermal resistance, °C/W - toplinski otpor	g	- acceleration due to gravity, ms ⁻² - gravitacija
$k_{cu,ir}$	- equi. conductivity coefficient, W/m/°C - ekvivalentni koeficijent vodljivosti	c_p	- fluid specific heat capacity, kJ/kg/°C - specifični kapacitet fluida
t_{eq}	- equivalent air thickness, m - ekvivalentni zračni sloj	h	- heat transfer coefficient, W/m ² /°C - koeficijent prijelaza topline
A_{slot}	- interior slot area, m ² - unutarnja površina utora	μ	- fluid dynamics viscosity, kg/(s·m) - viskoznost fluida
S_{slot}	- stator slot area, m ² - površina utora statora	ρ	- fluid density, kg/m ³ - gustoća fluida
S_{cu}	- copper surface in the stator slot, m ² - površina bakra u utoru statora	β	- dynamic viscosity, Pa·s - dinamička viskoznost
l_{sp}	- stator slot perimeter, m - perimetar utora statora		
Re	- Reynolds number - Reynoldsov broj		
Gr	- Grashof number - Grashof broj	Indices/Indeksi	
Nu	- Nusselt number - Nusseltov broj	MIXED	- mixed heat transfer - miješani prijelaz topline
Pr	- Prandtl number - Prandtlvov broj	FORCED	- forced heat transfer - prisilni prijelaz topline
		NATURAL	- natural heat transfer - prirodni prijelaz topline

The circuit, shown in Figure 1, is a three dimensional representation of the main heat transfer paths within an induction motor. Thermal resistances for the conduction heat transfer paths are calculated from the dimensions and thermal conductivity of each component. Radiation is calculated using emissivity and view factor coefficients and component surface area. Convection thermal resistances (natural and forced) are calculated using proven empirical correlations which are based on dimensional analysis [5].

2. Various thermal aspects

2.1. Interface gaps between components

The accuracy of a motor thermal performance prediction is dependant upon the estimate of the many thermal contact resistances within the machine e.g. stator lamination to housing, slot-liner to lamination, etc. A contact resistance is due to imperfections in the touching surfaces and is a complex function of material hardness, interface pressure, smoothness of the surfaces and air pressure. The easiest way to deal with thermal contact resistances in a design algorithm is to base the thermal resistance on an average interference airgap. For the typical material interfaces found in electrical

machines we find values of interface gap for aluminum-iron of 0,0006 mm to 0,006 mm. We can use these values as first estimates of interface gaps in electrical machine analysis.

Two gaps that we must look at in more details are the lamination to housing interface gap and the gap between slot-liner and lamination. The gap between lamination and housing is a function of how well the rough laminated outer surface of the stator is prepared before the housing is fitted. A further complexity is that often there are other features stamped into the outer surface of the lamination to housing interface which effectively gives an increased gap. Also, if that housing is made from aluminum then due to its relative softness compared to a cast iron frame this should lead to a reduced effective gap. The problem is that the difference in thermal expansion rates between it and the stator lamination gives rise to an increasing effective gap at high temperatures – often eliminating the softness advantage. Complexities in the slot-liner to lamination interface are that the liner material is quite pliable, the slot surface is laminated, the gap may be filled or partially filled with impregnation and a large slot-fill will tend to push the liner towards the lamination.

A value of lamination to housing interface gap found by experimentation on a 4 kW TEFC induction machine

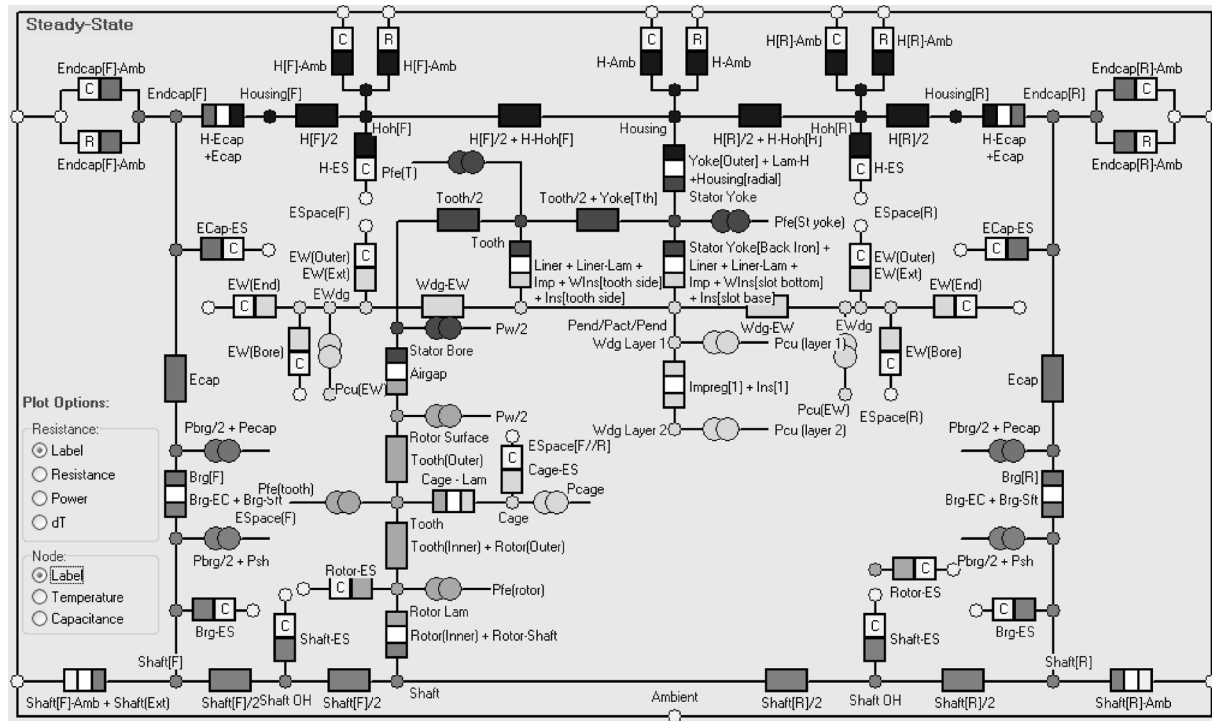


Figure 1. Lumped Circuit for an induction motor thermal model
 Slika 1. Električna shema toplinskog modela asinkronog stroja

[6] was 0,042 mm. But this value can vary significantly depending upon the manufacturing process and materials used. Values of between 0,01 mm and 0,08 mm have been measured on other TEFC induction motors.

2.2. Winding models

In electrical machines that have random wound mush winding, it is neither possible, nor desirable, to model the position of each individual conductor when carrying out thermal analysis. Even when using precision and form wound windings, it is not necessary to model each individual conductor to predict the temperature distribution accurately. End windings have in many cases a more random nature than the active section of the motor.

The use of a composite thermal conductivity is often used to predict the heat transfer and temperature distribution within a winding [6]. Such simple analytical equations can easily be included in a lumped circuit program. This does, however, present a problem in that it is difficult to base the composite thermal conductivity calculation on the slot geometry and amount of materials in the slot, i.e. to find a suitable and reliable method to determine the equivalent thermal conductivity $k_{cu,ir}$ of the air and insulation material in the slots and to set a value for conduction path length and area based on slot geometry. This equivalent thermal conductivity depends

on several factors, such as material and quality of the impregnation, residual air quantity after the impregnation process and so on. If the equivalent thermal conductivity $k_{cu,ir}$ is known the thermal resistance between the winding and the stator lamination can be computed using the following equation:

$$R_{cu,ir} = \frac{t_{eq}}{k_{cu,ir} A_{slot}}, \tag{1}$$

t_{eq} - equivalent thickness of the air and all the insulation material in the stator slots;

$k_{cu,ir}$ - equivalent conductivity coefficient of the air and insulation material in the stator slots, evaluated by DC supply experimental test;

A_{slot} - interior slot area ($A_{slot} = l_{sb} L_s$).

$$t_{eq} = \frac{S_{slot} - S_{cu}}{l_{sp}}, \tag{2}$$

S_{slot} - stator slot surface, m^2

S_{cu} - copper surface in the stator slot, m^2

l_{sp} - stator slot perimeter, m.

One formulation that has been published for the equivalent thermal conductivity is [6]:

$$k_{cu,ir} = 0,1076 * k_f + 0,029967, \tag{3}$$

where the value of $k_{cu,ir}$ equal to the air thermal conductivity for a filling factor k_f equal to zero has been imposed.

Taking into account that the filling factor used in the tested TEFC induction motor is 0,42, the equivalent thermal conductivity is 0,075 acc. [6].

There was an added requirement for the winding model to be incorporated in Motor-CAD, in that it needed to be very simple to understand and visualize the results. To achieve this, a new method was developed based on a layered winding model. A depiction of the model is shown in Figure 2. In the model we try to lump conductors together that have a similar temperature. Layers of copper that have roughly equal temperature are expected to be a similar distance from the lamination. The layers start at the slot boundary with a lamination to slot liner interface gap (this can be an air/impregnation mixture), then a slot liner (known thickness) and then layers of impregnation, wire insulation and copper.

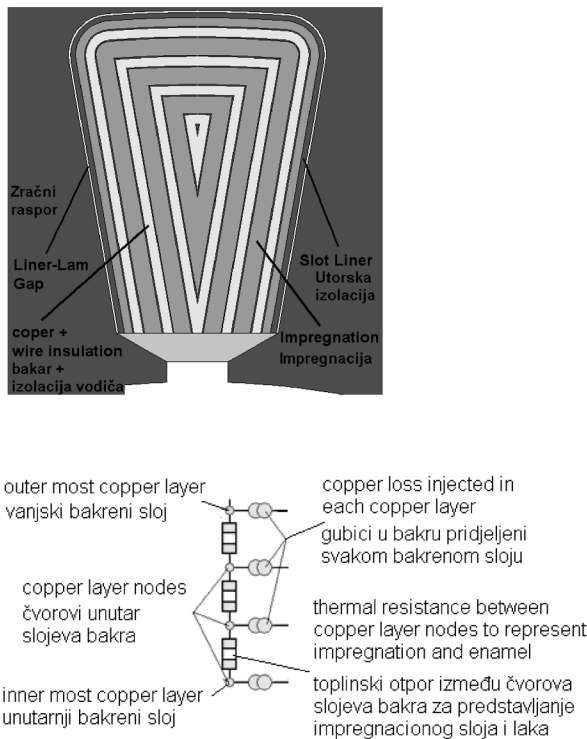


Figure 2. Layered winding model suitable for electric machines

Slika 2. Slojeviti model namota za električne strojeve

It is assumed that heat transfer is through the thickness of the layers. The series of thermal resistances are shown in Figure 2. It is easy to calculate the resistance values from the layer cross-sectional area (A), thickness (l) and material thermal conductivity (k), i.e. $R_t = l/(A \cdot k)$. For a given slot fill, if small strands of wire are selected then more conductors result. In such cases one would expect

more effective gaps between conductors and so have more copper layers. To achieve this we make the copper layer thickness equal to that of the copper diameter. The winding algorithm then iterates with the spacing between copper layers until the copper area in the model is equal to that in the actual machine. This sets the number of copper layers. The slot area left after inserting the liner and copper layers is copper insulation and impregnation. A similar constraint is also placed on the wire insulation in that the model insulation area is equal to that in the real machine. The only other parameter that needs be set in the model is the thickness of the first layer of impregnation in comparison to the rest. The default value used in the program is half the thickness of the other layers. This is because typically many of the round conductors will be in contact with the liner surface.

The beauty of the model is that we can simply apply impregnation goodness factors to analyses the effect of air within the impregnation using a weighted sum of impregnation and air thermal conductivity. Typically larger impregnation goodness factors can be achieved with vacuum impregnation rather than trickle or dip varnish processes [2].

2.3. Convection from housing surface

Within the heat transfer technical literature there exists many empirical correlations that are suited to the prediction of convection cooling from surface shapes typically seen in electrical machines [7-9]. For instance correlations exist for natural and forced convection from simple shapes such as cylinders and flat plates and more complex structures such as open and closed channels of various shapes and sizes. Such correlations are usually based on the dimensionless numbers: Reynolds (Re), Grashof (Gr), Prandtl (Pr) and Nusselt (Nu) numbers. For natural convection the typical form of the correlation is:

$$Nu = a (Gr \cdot Pr)^b \quad (4)$$

For forced convection the typical form is:

$$Nu = a (Re)^b (Pr)^c \quad (5)$$

where a , b and c are constants given in the correlation. Also:

$$Re = \rho v L / \mu, \quad (6)$$

$$Gr = \beta g \Delta T \rho^2 L^3 / \mu^2, \quad (7)$$

$$Pr = c_p \mu / k, \quad (8)$$

$$Nu = h L / k, \quad (9)$$

h - heat transfer coefficient, $W/(m^2 \cdot K)$

μ - fluid dynamic viscosity, $kg/(s \cdot m)$

ρ - fluid density, kg/m^3

k - fluid thermal conductivity, W/(m·k)

c_p - fluid specific heat capacity, kJ/(kg·k)

v - fluid velocity, m/s

ΔT - delta temperature of surface-fluid, (k)

L - characteristic length of the surface, m

β - fluid coefficient of cubical expansion
 $1/(273 + T_{\text{FLUID}})$, (1/k)

g - gravitational force of attraction, m/s²

The magnitude of Re is used to judge if there is laminar or turbulent flow in a forced convection system. Similarly the $Gr \cdot Pr$ product is used in natural convection systems. Turbulent flows give enhanced heat transfer but added resistance to flow in a forced convection system.

The parameter that we are ultimately seeking is h . Once we know h we can calculate a thermal resistance to put in the lumped circuit model using the relationship:

$$R = \frac{1}{Ah} \quad (10)$$

Natural convection heat transfer is a primary function of the temperature difference between component and fluid and the fluid properties. Forced convection is a primary function of the fluid velocity and fluid properties and the only secondary function of the temperature in those fluid properties are temperature dependent. It is often easier to predict the heat transfer due to natural convection as we do not need to predict the local fluid velocity. This is usually true in machines intended for natural convection as they either have relatively smooth well defined surfaces or include radial fins that are intended for natural flow in the inter-fin channels. For such cases well-proven correlations exist. Cases where the natural convection calculation is more complex are in TEFC machines where the use of axial fins do not lend themselves to inducing a good flow of naturally convected air deep into fin channels. We must, however, be able to predict the natural heat transfer in such machines as motors with shaft mounted fans are often operated close to stall at which point natural convection dominates. Special formulations have been developed for use in Motor-CAD to give an accurate calculation in such situations. Area based composite correlations are used for the complex finned shapes with each part of the geometry using a correlation that is best suited to its shape and orientation, i.e. a combination of vertical flat plate, horizontal flat plate (upper and lower facing), cylinder and horizontal fin channel correlations. Also, terms are introduced to limit the dissipation area to a depth down the fin channel equal to fin spacing as there will be little air circulation at the base of deep narrow axial channels fitted to the sides of a motor. A special form of average is used so that if the fins are deep compared to spacing

then the fin side correlation predominates, but if the fins are not deep then the fin base correlation predominates. The results obtained show that a good prediction of the natural convection can be achieved using such complex correlations. The calculated data is for Motor-CAD with default setting of all parameters – all the user has done is to input the geometry for the motor and its foot mounting (the cooling from the flange or foot mounting is important and is included in the analysis), the winding details, the materials and the losses. For the 4 kW induction motor natural convection resistance given in [6] is 0,275 °C/W obtained by test and 0,26 °C/W obtained by Motor-CAD.

The mixed heat transfer due to the combination of natural and forced convection is estimated using the formulation [5]:

$$h_{\text{MIXED}}^3 = h_{\text{FORCED}}^3 \pm h_{\text{NATURAL}}^3 \quad (11)$$

where the motor orientation determines the \pm sign used, a + sign for assisting and transverse flow and a – sign for opposing flows.

A. Open fin channel blockage and leakage

In TEFC machines with open fin channels the prediction of the local fluid velocity is often complicated by the fact that there is a tendency for air not to stay within the channels, i.e. leakage reducing the velocity of air in channels away from the fan exit. Some channels may be blocked by such features as terminal boxes and lifting lugs. Motor-CAD includes channel blockage and leakage factors to aid the user in determining accurate velocities. In the correlation it is assumed that the flow is always turbulent due to the fact that the radial fans and cowlings used in such machines create turbulence.

The inlet velocity to the fin channels is estimated by using empirical data given in [6]. The average velocity of the air in the fin channels as it leaves the fan is close to 6 m/s. The actual variation in velocity from channel to channel can vary significantly and is a function of the fan direction, as shown in Figure 3. Alternatively we may know the volume flow rate. As we know the channel dimensions and the inside diameter of the cowling we can calculate the velocity from the cross-sectional area available for flow.

The prediction of the actual reduction in velocity is a complex function of many factors including the fan, fin and cowling design and rotational speed. Here we have taken the default parameters in Motor-CAD and calculated the effective thermal resistance between housing and ambient. The open channel air leakage data is used as default in this case. It is seen that an accurate estimate can be made if the user has a basic knowledge of the inlet air velocity or volume flow rate to the fin channels. Fin blockage is simply accounted for by the

user counting the total number of fin channels (N_{total}) and the blocked channels N_{block} . The factor used is then:

$$\frac{N_{total} - N_{block}}{N_{total}} \quad (12)$$

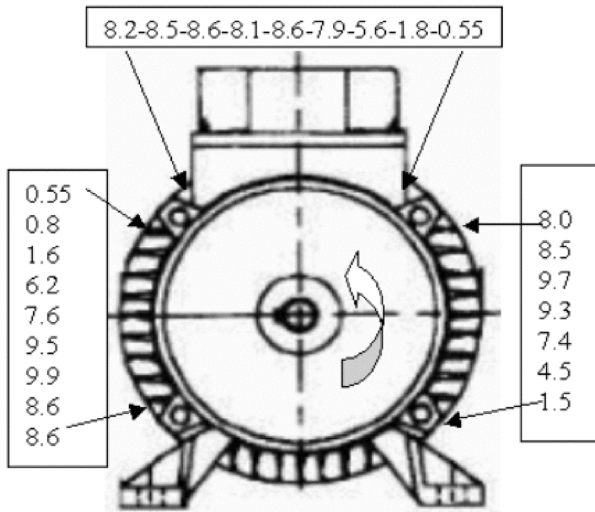


Figure 3. Typical form of variation in fin channel air velocity with fin position (reported speed in m/s)

Slika 3. Tipični oblik promjene brzine rashladnog zraka u kanalima između rashladnih rebara (prikazana brzina u m/s)

2.4. End space cooling

The end-space is defined as the area within the end-shields that contains the end winding, end-cage (in induction machines) and any simple fans. This area of machine cooling is renowned as being one of the most difficult to predict accurately. This is because the fluid flow (air in most cases) in the end space region of an electric motor is usually much more complex than that for flow over its outer surfaces. The flow depends on many factors including the shape and length of the end winding, added fanning effects due to wafers/wands, the surface finish of the end sections of the rotor and turbulence. Notwithstanding the complexity, several authors have studied the cooling of internal surfaces in the vicinity of the end-winding [6]. Some have based their results on testing and some on CFD. In the majority of cases they propose the use of a formulation of the form:

$$h = k_1 \left(1 + k_2 v_{el}^{k_3} \right), \quad (13)$$

h - heat transfer coefficient, W/(m²·k)

k_1, k_2, k_3 - curve fit coefficients

v_{el} - local fluid velocity, m/s.

The " $k_1 * I$ " term accounts for natural convection while the " $k_1 * k_2 * v_{el}^{k_3}$ " term accounts for the added forced

convection due to rotation. Figure 4 compares published correlations for end-space cooling, where relatively good correspondence is shown for such a complex phenomena. The accuracy of CFD in predicting the local heat transfer is not guaranteed, but it is usually good at predicting local velocity variations [10]. This information can be usefully employed by analytical packages such as Motor-CAD to give more accurate models.

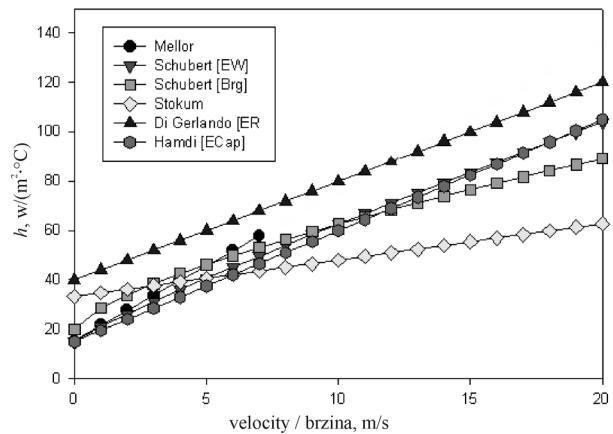


Figure 4. Published End Space Convection Correlations
Slika 4. Prikaz korekcijskih korelacija u čeonom prostoru

2.5. Airgap heat transfer

The traditional method for accounting for heat transfer across airgaps in electrical machines is to use the dimensionless convection correlation developed from testing on concentric rotating cylinders. In the analysis use is made of the Taylor (Ta) [11] number to judge if the flow is laminar, vortex or turbulent:

$$Ta = Re \sqrt{\frac{l_g}{R_r}}, \quad (14)$$

$$Re = \frac{l_g v}{\mu}. \quad (15)$$

The flow is laminar if $Ta < 41$. In this case $Nu = 2$ and heat transfer is by conduction only. If $41 < Ta < 100$ the flow takes on a vortex form with enhanced heat transfer:

$$Nu = 0,212 Ta^{0.63} Pr^{0.27} \quad (16)$$

If $Ta > 100$ the flow becomes fully turbulent flow and a further increase in heat transfer results:

$$Nu = 0,386 Ta^{0.5} Pr^{0.27}, \quad (17)$$

where:

R_r - rotor radius, m

l_g - airgap length, m.

The problem with the above formulation is that the slot opening is not included. Published data that includes saliency is quite scarce. Gazley [12] does look at slot-opening and finds that if the flow is laminar then there is a decrease in heat transfer compared to the smooth airgap. If the slots are on the rotor then the reduction is by around 10 %. If the slotting is on both surfaces the decrease can be as large as 20 %. If the flow is turbulent then there can be a significant increase in heat transfer. In the vortex flow range there is little difference to that of the smooth cylinder.

2.6. Material data

A thermal model is only as good as the material data put into it. There are a number of common deficiencies associated with data for materials used in electrical machines. One of the main deficiencies is the lack of thermal data provided by steel manufactures - typically they do not publish thermal conductivity data for silicon iron. As can be seen from Fig 5, the thermal conductivity is a function of the silicon content [13-17]. Steel manufactures also tend not to publish the chemical makeup of the steel.

The difference in lamination stack radial and axial lamination conductivities is an area that requires more research. The effective axial thermal conductivity is a complex function of such aspects as the clamping pressure, lamination thickness, stacking factor, lamination surface finish and interlamination insulation material [13,15]. Typical ratios of radial to axial thermal conductivity are 20 to 40.

Obtaining thermal conductivity data for critical materials such as the slot liner and impregnation can also be difficult. This situation is, however, improving with time as more motor manufactures ask for such data from component suppliers. Also there have been developments in improved insulation systems which have higher thermal conductivities. In such cases their thermal properties are published as they are selling points for the materials.

2.7. Bearings and end-shields

The bearing thermal model is not a simple problem. The bearing is a complex mechanical component from the thermal point of view. In particular, the balls are in contact with the inner and outer rings just in a very small mechanical spot and as a consequence, the thermal transfer is difficult to predict accurately. In addition inside the bearing the presence of grease and lubricant introduce new factors of uncertainty for thermal resistance determination. A simple solution is to consider the bearing as an equivalent interface gap - this method is used in Motor-CAD. The procedure is described in [6].

The obtained results seem to be interesting even if the test has been made with the rotor and the bearing at stall. In particular, these first results show that a bearing equivalent interface gap equal to around 0,3 mm can be considered in a thermal model first approach. If the predicted bearing temperature contact resistance difference is to be predicted with good accuracy, it is evident that an accurate model of the motor end shields is also required. It is possible to predict both radial and axial thermal resistance values for the end shields if we know their effective lengths and cross-sectional areas, $R_t = k/(A \times l)$. However, this process is sometimes complicated by the fact that the end shields can have complex shapes. We also have to take account of the interface fit to the housing.

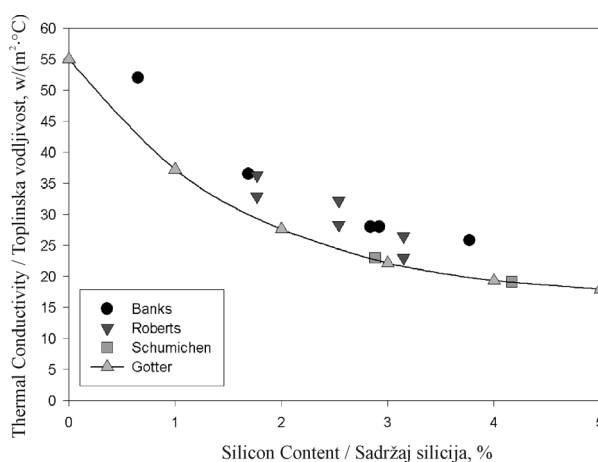


Figure 5. Variation of thermal conductivity with lamination silicon content

Slika 5. Promjena toplinske vodljivosti limova jezgri u ovisnosti o sadržaju silicija

3. Applications

The four-pole induction squirrel cage electrical motor that is considered here is shown in Figure 6. It has a 2,5 kW rating, is delta connected and has a 400 V, 50 Hz supply.

3.1. Steady state temperature calculation

The first part of the thermal analyses deals with the induction motor steady state temperature prediction. Input values to the Motor-CAD program are the geometry of the motor, winding details, material characteristic, cooling method and loss data. The motor losses are obtained by measurement and are given in Table 1. The calculated and measured temperature results are reported in Table 2.



Figure 6. TEFC motors used to generate test data

Slika 6. TEFC asinkroni stroj za provedbu eksperimentalnih testova

Table 1. Loss Data (W)

Tablica 1. Gubici (W)

TOTAL/UKUPNO	429
Stator Copper/Bakar statora	201
Stator Iron/Željezo statora	107
(Friction + Windage)/(Trenje + ventilacija)	22

NOTE:

(1) Friction (5+5) W, Windage 12 W

(2) The rotor losses is: 429-201-107-22 = 99 W = Loss rotor copper (89 W) + Loss rotor tooth (10 W)

Table 2. Calculated and measured temperatures (°C) at ambient temperature 22,4 °C

Tablica 2. Proračunate i mjerene vrijednosti temperature (°C) za temperaturu okoline 22,4°C

	Measure./ Mjerenje	Calcul./ Proračun	Differ./ Razlika
T (stator winding) * /(namot statora)	68,2	67,0	1,8 %
T (housing) * /(kućište)	51,6	50,1	2,9 %
T (rotor bar surface, midle of stack length) * /(površina štapa rotora, sredina paketa)	89,1	83,6	6,2 %
T (rotor bar, 10 mm axially from end ring on the outer rotor surface)* / (štap rotora, 10 mm aksijalno od krajnjeg prstena na površini rotora)	86	83,6	2,8 %
T (end ring)* / (krajnji prsten)	76,9	83,6	-8,7 %

* The temperature is measured by Thermocouple probe Copper-Constantan / temperatura je mjerena termoelementom bakar-konstantan

3.2. Transient temperature calculation

The second part of the thermal analyses deal with temperature prediction for a classical locked rotor test using a three phase sinusoidal supply. The safe stall point represents the maximum time the machine can stay locked without damage at a referenced starting voltage. Safe stall points are typically provided for low-voltage motors. NEMA MG-1 requires motors 500 HP and below with a rated voltage not exceeding 1kV which should be capable of withstanding locked-rotor current for not less than 12 seconds when the motor is initially at normal operating temperatures.

In this condition the mechanical losses are zero because the rotor speed is zero. The active losses are the stator and rotor ones only. The rotor losses can be computed from input power minus stator joule losses, as given in the following equation:

$$P_{jr} = P_{input} - 3 R_s I_s^2$$

The locked rotor loss values are given in Table 3.

Table 3. Locked rotor Loss (W)

Tablica 3. Gubici za zakočeni rotor (W)

TOTAL/UKUPNO	11145
Stator Copper/Bakar statora	5148
Rotor winding/Namot rotora	5997

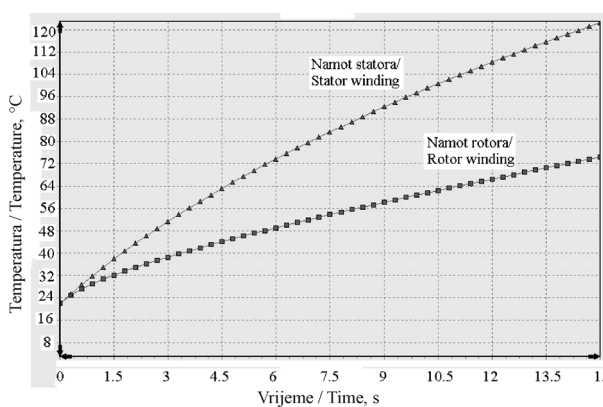


Figure 7. Calculated temperature versus time (locked rotor)

Slika 7. Proračun temperature u funkciji vremena (zakočen rotor)

The calculating locked rotor temperature versus time characteristic for stator and rotor winding respectively are shown in Figure 7.

The calculated and measured temperatures after 15 seconds of the locked rotor condition are reported in Table 4.

Table 4. Calculated and measured temperatures (°C) after 15 seconds locked rotor (22,4 °C ambient temperature)

Tablica 4. Proračunate i mjerene vrijednosti temperatura nakon 15 s za slučaj zakočenog rotora (22,4 °C temperatura okoline)

	Measure./ Mjerenje	Calcul./ Proračun	Diff./ Razlika
T (stator winding)* / (namot statora)	115	122	-5,7 %
T (rotor bar surface, middle of stack length)* /(površina štapa rotora, sredina paketa)	73	74	-1,4 %

* The temperature is measured by Thermocouple probe Copper-Constantan / temperatura je mjerena termoelementom bakar-konstantan

4. Conclusions

In this paper some of the more difficult aspects of electric motor thermal analysis are discussed. A steady-state and transient thermal model for induction machines is introduced. The model is included in the analytical design program Motor-CAD™ developed for the thermal analysis of electric motors and generators. Empirical data, based on previous testing on a large range of machines, is embedded into the software. This is to allow accurate prediction of manufacturing issues such as interface thermal resistance between stator lamination and housing, winding impregnation goodness, end winding convection cooling, axial fin channel air leakage, bearing heat transfer, etc. This enables a good level of accuracy of the thermal model without the need for calibration using test data on the actual machine under consideration. Measurements made on a test machine, with default values set for manufacturing parameters in Motor-CAD show that the thermal model offers a good level of accuracy. This enables a much better accuracy in an overall electromagnetic/thermal performance calculation and so allows the machine to be fully optimized without having to build in large safety margins to allow for uncertainty in thermal performance prediction.

REFERENCES

- [1] MELLOR, P.; ROBERTS, D.; Turner, D.: *Lumped parameter thermal model for electrical machines of TEFC design*, IEE Proceedings, Vol. 138, September 1991.
- [2] STATON, D. A.: *Thermal Computer Aided Design - Advancing the Revolution in Compact Motors*, IEEE IEMDC 2001, Boston, USA, June 2001.
- [3] STATON, D.; Pickering, S. J.; Lampard, D.: *Recent Advancement in the Thermal Design of Electric Motors*, SMMA 2001 Fall Technical Con., Durham. North Carolina, 3-5 Oct. 2001.
- [4] STATON, D.: *Thermal analysis of electric motors and generators*, Tutorial course, IEEE IAS Annual Meeting 2001, Chicago, USA
- [5] INCROPERA, F. P.; DEWITT, F. P.: *Introduction to Heat Transfer*, Wiley, 1990.
- [6] STATON, D.; BOGLIETTI, A.; Cavagnino, A.: *Solving the More Difficult Aspects of Electric Motor Thermal Analysis*, IEMDC 2003, 1-4 June 2003, Madison Wisconsin, USA.
- [7] HOLMAN, J. P.: *Heat Transfer*, McGraw-Hill, 1997.
- [8] MILLS, A. F.: *Heat Transfer*, Prentice Hall, 1999.
- [9] JANNA, W. S.: *Engineering Heat Transfer*, Van Nostrand Reinhold (International), 1988.
- [10] PICKERING, S. J.; LAMPARD, D.; HAY, N.; ROYLANCE, T. F.: *Heat transfer from end-windings of a low voltage concentric-wound induction motor*, IEE EMD 1995, UK, Sept 1995.
- [11] TAYLOR, G. I.: *Distribution of Velocity and Temperature between Concentric Cylinders*, Proc Roy Soc, 1935, 159, PtA, 546-578.
- [12] GAZLEY, C.: *Heat Transfer Characteristics of rotating and axial flow between concentric cylinders*, Trans ASME, Jan (1958), 79-89.
- [13] PAL, S. K.: *Heat Transfer in Electrical Machines – A Critical Review*, ERA Report No 71-76, July 1971.
- [14] GOTTER, G.: *Heating and cooling of electrical machines*, 1954, Springer-Verlag, Berlin – In German.
- [15] ROBERTS, T. J.: *Determination of the thermal constants of heat flow equations of electrical machines*, Proc IME, 1969-70, Vol 184, Pt 3E, 84-92.
- [16] BANKS, P. J.: *Thermal conductivity of sheet steel laminations*, AEI Manchester Report No.TP/R/1,188, 1961.
- [17] SCHUMICHEN, M.: *Longitudinal and transverse thermal conductivity of laminated transformer sheets*, Elektrische, 20(1966)12. In German.